Langmuir

Article

pubs.acs.org/Langmuir

One Pot Synthesis of $Mg_2Al(OH)_6Cl{\cdot}1.5H_2O$ Layered Double Hydroxides: The Epoxide Route

Víctor Oestreicher[†] and Matías Jobbágy*[,†,‡]

[†]INQUIMAE-DQIAQF, Facultad de Ciencias Exactas y Naturales, Universidad de Buenos Aires, Ciudad Universitaria, Pab. II, C1428EHA, Buenos Aires, Argentina

[‡]Centro Interdisciplinario de Nanociencia y Nanotecnología, Buenos Aires, Argentina

Supporting Information

ABSTRACT: Pure $Mg_2Al(OH)_6Cl{\cdot}1.5H_2O$ layered double hydroxide (LDH) has been synthesized at room temperature by a one-pot method, homogeneously driven by chloride-assisted glycidol rupture (epoxide route). Well-defined nanoplatelet texture was achieved and the LDH crystallization mechanism discussed. Nanoplatelets self-assemble in the form of highly oriented films with excellent optical properties. LDH films exhibited stability toward detaching in aqueous solutions and allowed a fast anionic exchange preserving a high transparency.

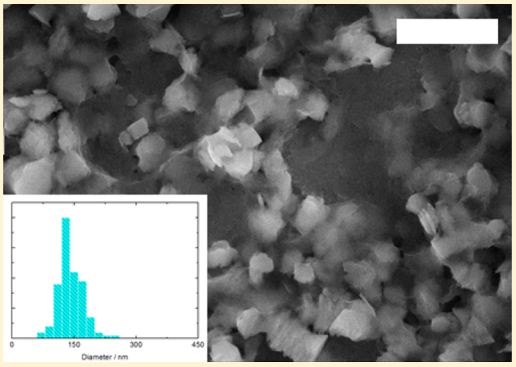

INTRODUCTION

Layered double hydroxides (LDHs) intercalated with exchangeable anions are well-established materials for sorption, intercalation, and the preparation of hybrid phases. In particular, single crystalline LDHs intercalated with certain anions were demonstrated to be outstanding phases to develop massive exfoliation or delamination, employing polar solvents under mild conditions.[1,2] The resulting stable suspensions of true two-dimensional LDH crystals hold a great potential in the field of nanotechnology,[3] since they deliver these nanobuilding blocks for the preparation of highly oriented self-assembled films,[4] layer by layer assemblies, and nanoshells,[5] still preserving their inherent intercalation chemistry, giving birth to a new family of advanced materials.[6−8] However, these compounds, in contrast with other layered solids as titanates,[9] have an inherent thermal instability that hinders crystallization through annealing procedures, limiting their obtainment to solution-based procedures.[10−13] The homogeneous precipitation method, based on the in situ controlled alkalinization, favors the occurrence of well-defined single crystalline particles with low size dispersion. In particular, urea hydrolysis successfully produced single crystalline LDH platelets bearing high aspect ratio, composed of Al(III) and Mg(II) or several divalent transition metals, in the carbonate form exclusively.[14−19] However, this method requires a temperature higher than 343 K and involves undesired intermediaries, as OCN^- and/or by products as carbonate.[3] The latter irreversibly intercalates within the LDH particles imposing an acid driven exchange treatment in order to achieve any desired exchangeable form, including the chloride one.[20−23] Very recently, a moderate thermal hydrolysis of hexamethylenetetramine (HMT)[24] allowed the straight crystallization of nitrate forms of several Al(III)-based LDHs preventing the incorporation of carbonate.[25] However, one of the most relevant LDH phases, the Mg(II)−Al(III) one, was not possible to obtain, except in the carbonate form.[25] In recent years, several reports have illustrated how epoxides are able to drive homogeneous alkalinization of aqueous solutions under mild temperatures. The process is based on the protonation of the oxo bridge with a subsequent nucleophilic attack, typically driven by chloride, resulting in the ring-opening and a net hydroxyl release.[26,27] This method was extensively employed for the preparation of several hydrogels at room temperature, leading to the so-called non-alkoxide sol gel process. The reaction proceeds with several cations,[28,29] ranging from transition metals[30−33] to rare earths.[34]

The present study demonstrated how this reaction allows for the very first time the straight synthesis of single-crystalline particles of chloride from of Mg(II)−Al(III) LDH at room temperature. The main synthesis parameters as well as the crystallization mechanism are discussed. Taking advantage of the textural properties of these particles, their aqueous suspensions were deposited onto glass substrates and self-assembled in the form of highly oriented films with excellent optical properties.

Received: June 14, 2013
Revised: July 30, 2013
Published: September 5, 2013

EXPERIMENTAL SECTION

Synthesis and Chemical Characterization of Solids. Typically, precipitations were driven by aging at 298 K 100 cm^3 of filtered solutions containing NaCl (50−750 mM), glycidol (50−500 mM), a salt of Mg(II) (6.6−8.0 mM), and Al(III) (2.0−3.3 mM) adjusted at pH = 3.0 with HCl. For certain experiences, total cationic content as well as the Al(III) to Mg(II) ratio was modified. After increasing aging times, ranging from hours to weeks, the precipitated solids were collected by ultracentrifugation, washed three times with filtered cold Milli-Q water, and dried at room temperature. Despite the numerous reports dealing with ethylene oxide-driven alkalinization,[30−34] glycidol was chosen due to its higher boiling point, which makes it easy to handle at room temperature, preventing losses due to evaporation and eventual harmful inhalations.[35]

Precipitation pH Profiles. Representative precipitation curves were obtained by in situ potentiometric pH measurement in a reactor regulated at 298 K under permanent stirring. All samples were constantly purged with N_2, in order to prevent atmospheric CO_2 uptake.

Characterization of Solids. All synthesized solids were characterized by powder X-ray diffraction (PXRD) using a graphite-filtered Cu K_α radiation (λ = 1.5406 Å); crystalline size along the *00l* direction was estimated with Scherrer's equation employing 003 and 006 reflections. The samples were inspected by means of field emission scanning electron microscopy (FESEM), equipped with energy dispersive X-ray spectroscopy (EDS) probe. Both Mg(II) and Al(III), chloride, and water content were assessed by ICP, ionic chromatography, and elemental analysis, respectively.

RESULTS AND DISCUSSION

As a first step to tune the rate of precipitation reactions, glycidol rupture rates were evaluated at 298 K. In situ pH determination revealed that the initially low pH only rises after minutes, allowing the proper homogenization of all reagents, and in less than 1 h, pH rises over 10.0. Alkalinization performed under decreasing NaCl concentrations reproduced a similar profile, taking longer periods of time to reach alkaline conditions.

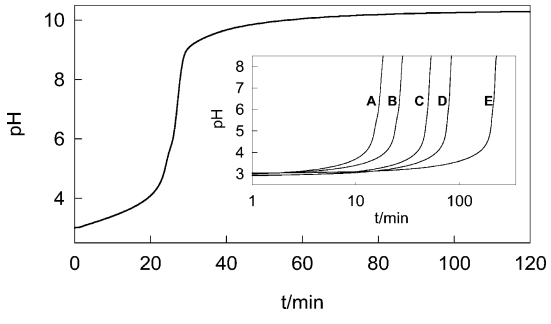

Figure 1. Evolution of pH at 298 K of aqueous solution containing 150 mM of glycidol and 750 mM NaCl. Inset: comparative evolution of pH at 298 K of aqueous solution containing 150 mM of glycidol and 750 (A), 450 (B), 250 (C), 150 (D), or 50 mM (E) of NaCl.

In order to compare the pH profiles observed under different initial NaCl concentrations, a precipitation time, $t_{pH=7.00}$, was defined as the necessary time for each NaCl-glycidol solution initially adjusted at pH 3.00 to reach the value of 7.00. The alkalinization profiles were revealed to be strongly dependent on both the initial NaCl and glycidol concentration (see Figure S1). However, once a reduced time, t^*, defined as $t/t_{pH=7.00}$ was employed as common time scale for all alkalinization runs, pH profiles were superimposable under the evaluated conditions. A similar behavior was found keeping NaCl concentration fixed at 50 mM, and increasing the glycidol concentration. Then, reduced times referred to the faster reaction were plotted as a function of concentration increment, for both variable NaCl or glycidol set of runs, revealing a first order law on each reagent under the concentration range explored herein (see Figure 2).

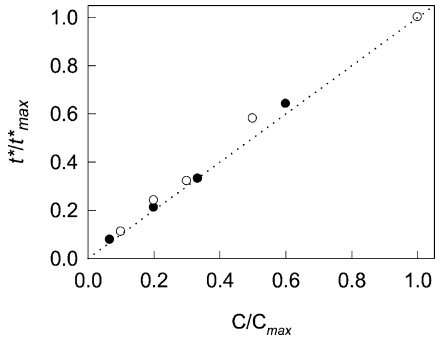

Figure 2. Dependence of the alkalinization rate, expressed as the ratio of t^* to t^*_{max}, with the increasing starting concentrations of NaCl (●) or glycidol (○), expressed as the ratio of concentration respect to the maximum one, C_{max}.

Once the alkalinization rate law was established, the precipitation process was also monitored in terms of pH evolution. As a first step to understand the formation of LDH phases, the precipitation behavior of each cation was inspected separately, employing low cationic concentrations according to well-established homogeneous procedures.[18] In the case of bare Al(III) solution, the pH profile shows a well-defined plateau around pH = 4.4, resulting in a translucent stable sol, typically obtained under mild conditions.[36] The sol coagulated at around pH 6.0, denoting a deceleration on the alkalinization profile, due to the final deprotonation of the remnant OH groups in good agreement with previous reports based on titration experiments,[37−40] PXRD analysis revealed an ill-crystallized $Al(OH)_3$ phase, with broad reflections positioned close to Bayerite ones (see Figure S2), typically observed from the assembly of keggin $Al_{13}O_4(OH)_{28}^{3+}$ cationic moieties.[36] After massive flocculation of this sol the pH increased to the final maximum value, close to 9.5, constrained by the remnant amount of epoxide. In contrast with Al(III) solutions, pure Mg(II) ones of similar concentrations remained undisturbed with no base consumption nor precipitation, reaching a maximum pH value close to 10.6, exhibiting a pH rise profile superimposable to chloride−epoxide control solution. However, once Mg(II) ion concentration was increased to 50 mM, a precipitation overshoot pH value close to 10.4 was observed, stabilizing the precipitation plateau at pH 10.2. The obtained phase consists of a mixture of single and polycrystalline hexagonal platelets of brucitic $Mg(OH)_2$ (see Figure S3). In the case of Mg(II)−Al(III) binary solutions, Al(III) cations precipitate in a first step, following the characteristic pH curve of bare Al(III) reference, indicating that this cation precipitates independently from the binary phase. A pH overshoot is registered after 17 h, reaching a value of 9.5 triggering a second precipitation plateau centered at pH = 9.33, well below the observed value for pure $Mg(OH)_2$ (see Figure S4),[39] and in excellent agreement with the solubility data recorded for Mg(II)−Al(III)−chloride LDHs.[41] Then, this second event, in which Mg(II) ions are consumed from solution at an almost constant pH value of 9.33, will be described as the LDH plateau in the following (Figure 3).

dx.doi.org/10.1021/la402260m | *Langmuir* 2013, 29, 12104−12109

Longer aging times (several days) exhibited a slight increase of pH up to a value of 9.5.

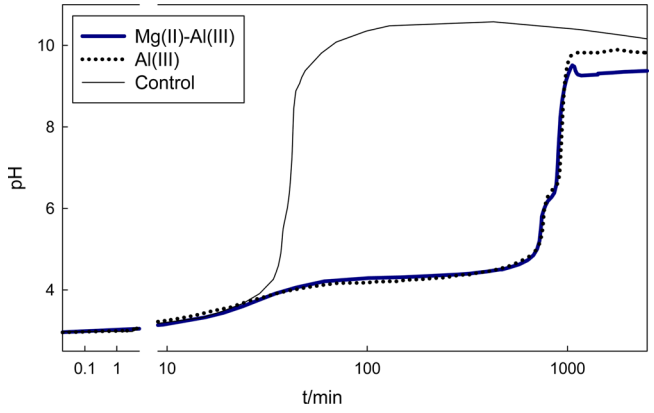

Figure 3. Time evolution of pH at 298 K for solution containing NaCl 100 mM, glycidol 400 mM, and $MgCl_2$ 6.6 mM (black thin line); $AlCl_3$ 3.3 mM (black dotted line), and $MgCl_2$ 6.6 mM + $AlCl_3$ 3.3 mM (blue line). Control alkalinization curve (NaCl 100 mM, glycidol 400 mM) was omitted since it is superimposed on the black thin line.

A detailed inspection of the phases obtained as a function of time was assessed in order to gain insight into the precipitation mechanism; Figure 4 depicts the PXRD patterns of solids collected after increasing aging times.

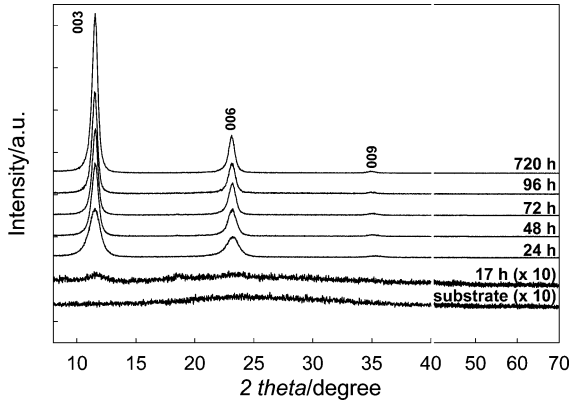

Figure 4. XRD patterns for solids obtained after increasing aging times solutions containing NaCl 100 mM, glycidol 400 mM, $MgCl_2$ 6.6 mM; and $AlCl_3$ 3.3 mM. All samples were deposited from their aqueous suspensions onto glass (substrate).

As soon as the overshoot takes place, ill-defined reflections of Mg(II)−Al(III) LDH are noticeable; just 7 h later, intense LDH reflections prevail. Further aging in mother liquors enhanced crystallinity; 00*l* reflection indicated that LDH particles, on average, grow up to 25 ± 5 nm in the *c* direction (see Figure 5). Further aging at 298 K does not imply crystalline growth, even after a 4-week-long period. The lack of other noticeable reflections than the interbasal 00*l* indicates a massive tendency among the LDH particles to develop oriented self-assembly guided by the flat surface of the glass substrate, expected for high-aspect-ratio single crystals (platelets). Samples deposited onto silicon wafers for FESEM inspection also developed a high degree of orientation (see Figure S5).The evolution of crystalline domain size along the *c* direction indicates that the LDH phase achieves both the definitive

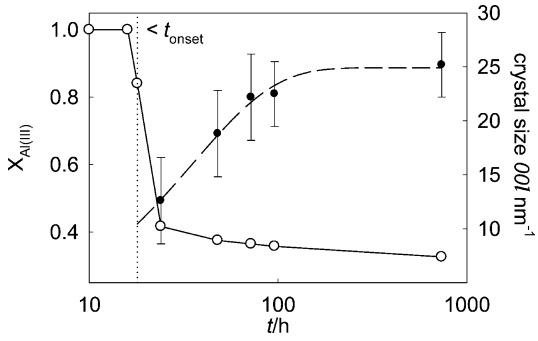

Figure 5. Evolution of Al(III) molar fraction of the solid phase (○) and LDH crystallite size along the 00*l* direction (●) as a function of time. Dotted line depicts the time of pH onset related to LDH heterogeneous nucleation.

thickness and the stoichiometric Mg(II) incorporation after ca. 100 h of aging once the precipitation is completed (see Figure 5).

FESEM inspection (Figures 6 and S6) of the samples revealed that soon after the pH onset, in the beginning of the

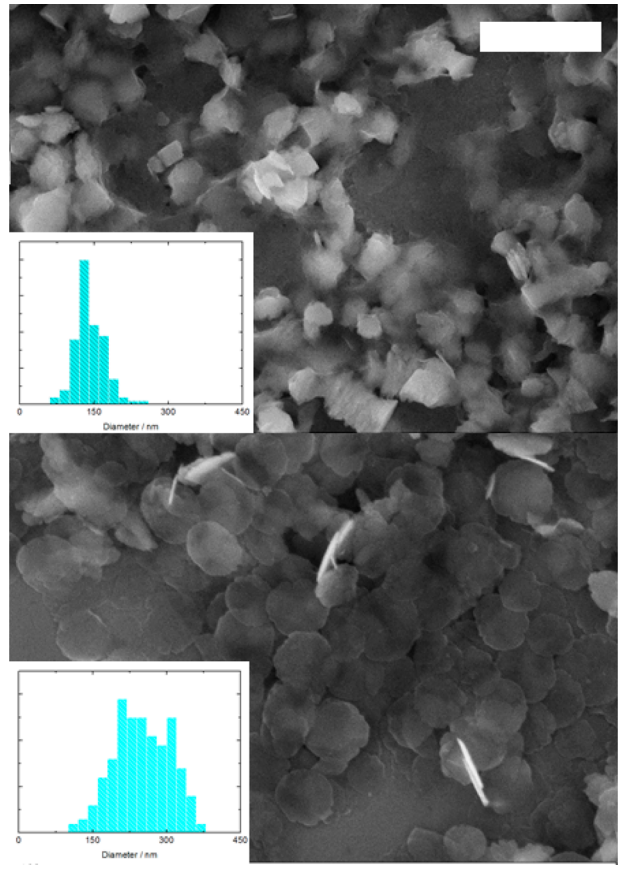

Figure 6. FESEM images of Mg(II)−Al(III) samples aged for 20 h (upper image) and 96 h (lower image). Scale bar represents 500 nm for both images.

LDH plateau, platelets of ca. 100 ± 30 nm in diameter coexist with large amounts of an amorphous phase, preserving the aspect of the parent $Al(OH)_3$ nanoparticles. The precipitation of Mg(II) cations ends after 96 h in parallel with $Al(OH)_3$ massive redissolution and LDH crystallization, in the form of larger single crystalline platelets defined around 250 ± 50 nm in

dx.doi.org/10.1021/la402260m | *Langmuir* 2013, 29, 12104−12109

diameter and 30 ± 5 nm in thickness, in good agreement with PXRD data. Further aging exert only a slight effect on the shape and size, suggesting that room temperature ripening is extremely slow for this system (see Figure S5).

An additional set of samples was repeated, increasing the Mg(II) to Al(III) ratios in the starting solutions keeping the total cation content constant. Chemical analyses of solid samples revealed the stable stoichiometry depicted in the formula $Mg_2Al(OH)_6Cl{\cdot}1.5H_2O$, irrespective of initial composition of the solution. PXRD patterns confirmed the presence of LDH phases, exclusively with a *c* cell parameter 23.1 ± 0.1 Å typical of the chloride LDH form,[42] confirming the inherent stability of that phase with respect to other stoichiometry, in agreement with other authors.[43] No traces of $Mg(OH)_2$ segregation were observed by PXRD while the remnant Mg(II) ions remained in solution. For Mg(II) to Al(III) ratios higher than 2, alkalinization curves denoted shorter Al(III) precipitation plateau, accelerating the LDH precipitation pH overshoot in several hours while the pH value of it as well as the LDH plateau remained unaltered (see Figure 7). Assuming

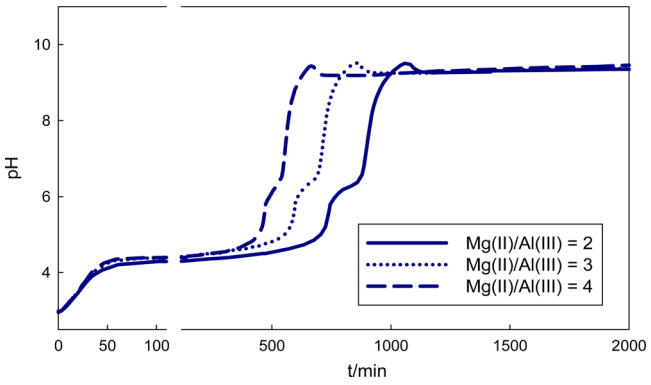

Figure 7. Precipitation curves for solutions containing NaCl 100 mM, glycidol 400 mM, and increasing Mg(II) to Al(III) ratio, keeping an initial total cation content of 10 mM, aged at 298 K.

that the formula that describes solubility equilibrium of growing LDH is $Mg_2Al(OH)_6Cl{\cdot}1.5H_2O$, and the concentration of free Al(III) is governed by already precipitated $Al(OH)_3$, all LDH precipitation curves obey a solubility product constant of ca. 2×10^{-51}, while the oversaturation value recorded during the overshoot is equal to 35 ± 5, irrespective of the initial Mg(II) concentration.

The transformation of pure Al(III) oxides into LDHs was documented in the past; even Al(III) oxides partially dissolve and coprecipitates with concomitant Me(II) cations in alkaline conditions at room temperature, in a process called surface precipitation.[44−46] However, in the present case, the inherent high solubility of nanometric parent $Al(OH)_3$ phase allows a massive transformation into the LDH phase. Since LDH overshoot is observed at a pH higher than the correspondent for $Al(OH)_3$ isoelectric point (pH 8−9),[47−49] the negative surface drives the adsorption of Mg(II) cations before LDH nucleation. The formation of single crystalline LDH particles of a much larger dimension than the parent $Al(OH)_3$ nanoparticles can be interpreted in terms of heterogeneous nucleation of single LDH crystals onto $Al(OH)_3$ nanoparticles. Once nucleation takes place, free chloride and Mg(II) ions in solution, the continuously generated hydroxyls, and the dissolution of remnant $Al(OH)_3$ nanoparticles feed the growth of LDH (see Scheme S1). An analogous mechanism was recently documented for the precipitation of hydrotalcite during the homogeneous precipitation with urea; however, under such energetic conditions, LDH phase develops from the dissolution of first precipitated nanoboehmite, AlO(OH).[50] In contrast with previous reports dealing with homogeneous procedures,[51] the present mild route develop platelets with the lack of central holes nor polycrystalline rosettes, suggesting that a single LDH nuclei grows onto nanometric $Al(OH)_3$ substrate that redissolves in a fast manner, preventing the aforementioned textural effects. As stated before, alkalinization rates can be increased proportionally either increasing chloride or glycidol initial concentrations; higher alkalinization rates favored smaller and better-defined particles of 180 ± 50 nm in diameter preserving a similar thickness and less degree of fracture damage (see Figure S6). A key property of highly oriented and dense LDH films lies in their good optical properties, that minimize light scattering, offering a suitable platform for hybrid photodevices.[52,53] To this aim, a thin film of LDH particles spontaneously assembled onto a glass substrate, in order to determine their absorbance due to scattering. The value recorded for the bare LDH film was very small; this film was submitted to an aqueous solution of an anionic dye, methyl orange (sodium 4-[(4-dimethylamino)phenyldiazenyl]-benzenesulfonate), in order to displace the chloride anions from the LDH interlayer. Minutes later, once exchange reaction was completed, the film acquired an homogeneous orange coloration, inherent to the intercalated dye, while the transparency of it remained unperturbed (see Figure 8), revealing a suitable stability toward resuspension, after being exposed to aqueous solution.

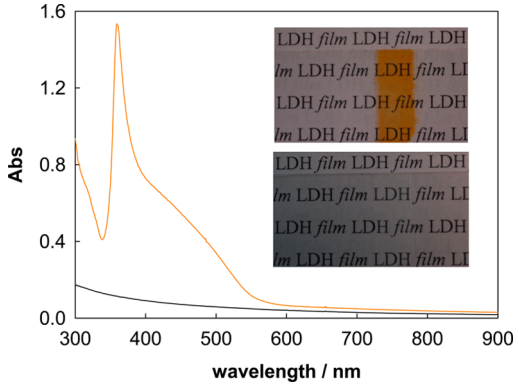

Figure 8. UV−vis absorbance spectrum of a LDH(Cl) film deposited onto a glass substrate from an aqueous suspension and the same film after being exchanged with methyl orange, LDH(MO). Inset: digital image of the former (bottom) and the latter (top).

The present study demonstrates that it is possible to obtain single crystalline particles of Mg(II)−Al(III) LDH in the exchangeable chloride form by means of a mild homogeneous alkalinization procedure based on glycidol's rupture. Alkalinization kinetics can be controlled either with chloride or glycidol concentration, up to a value of 10.5, offering a wider precipitation pH window with respect to ammonia releasing agents, that are intrinsically limited to a maximum pH value of 9.2, imposed by the NH_3/NH_4^+ buffer. In contrast, epoxide's rupture driven alkalinization allows the precipitation of very soluble phases, as $Mg(OH)_2$, offering a potential route for the preparation of several carbonate-free hydroxides or basic salts.

dx.doi.org/10.1021/la402260m | *Langmuir* 2013, 29, 12104−12109

The mild conditions employed in this route prevent primary particle ripening in a way that maximizes the preservation of the original nanoscopic dimension achieved in the earliest stages of precipitation and crystalline growth. Aqueous suspensions of these LDH particles spontaneously self-assemble in the form of robust films with good optical and exchange properties.

■ ASSOCIATED CONTENT

Supporting Information

PXRD, FESEM, and precipitation pH curves of reference $Mg(OH)_2$ and $Al(OH)_3$ solids. This material is available free of charge via the Internet at http://pubs.acs.org.

■ AUTHOR INFORMATION

Corresponding Author

*E-mail: jobbag@qi.fcen.uba.ar. Fax: 54-11-45763341.

Notes

The authors declare no competing financial interest.

■ ACKNOWLEDGMENTS

This work was supported by grants CONICET PIP 11220110101020 and UBACYT 20020100100636. M.J. is member of CONICET and Gabbos. VO wishes to thank ALN for the technical support.

■ REFERENCES

(1) Liu, Z.; Ma, R.; Ebina, Y.; Iyi, N.; Takada, K.; Sasaki, T. General synthesis and delamination of highly crystalline transition-metal-bearing layered double hydroxides. *Langmuir* **2007**, *23* (2), 861−867.

(2) Iyi, N.; Ebina, Y.; Sasaki, T. Water-swellable MgAl-LDH (layered double hydroxide) hybrids: Synthesis, characterization, and film preparation. *Langmuir* **2008**, *24* (10), 5591−5598.

(3) Wang, Q.; O'Hare, D. Recent Advances in the Synthesis and Application of Layered Double Hydroxide (LDH) Nanosheets. *Chem. Rev.* **2012**, *112* (7), 4124−4155.

(4) Liu, Z. P.; Ma, R. Z.; Osada, M.; Iyi, N.; Ebina, Y.; Takada, K.; Sasaki, T. Synthesis, anion exchange, and delamination of Co-Al layered double hydroxide: Assembly of the exfoliated nanosheet/polyanion composite films and magneto-optical studies. *J. Am. Chem. Soc.* **2006**, *128* (14), 4872−4880.

(5) Li, L.; Ma, R. Z.; Iyi, N.; Ebina, Y.; Takada, K.; Sasaki, T. Hollow nanoshell of layered double hydroxide. *Chem. Commun.* **2006**, *29*, 3125−3127.

(6) Yan, D.; Qin, S.; Chen, L.; Lu, J.; Ma, J.; Wei, M.; Evans, D. G.; Duan, X. Thin film of sulfonated zinc phthalocyanine/layered double hydroxide for achieving multiple quantum well structure and polarized luminescence. *Chem. Commun.* **2010**, *46* (45), 8654−8656.

(7) Xu, J.; Zhao, S.; Han, Z.; Wang, X.; Song, Y.-F. Layer-by-Layer Assembly of $Na_9[EuW_{10}O_{36}]\cdot 32H_2O$ and Layered Double Hydroxides Leading to Ordered Ultra-Thin Films: Cooperative Effect and Orientation Effect. *Chem.—Eur. J.* **2011**, *17* (37), 10365−10371.

(8) Yan, D.; Lu, J.; Ma, J.; Wei, M.; Evans, D. G.; Duan, X. Reversibly Thermochromic, Fluorescent Ultrathin Films with a Supramolecular Architecture. *Angew. Chem., Int. Ed.* **2011**, *50* (3), 720−723.

(9) Sasaki, T.; Watanabe, M. Osmotic swelling to exfoliation. Exceptionally high degrees of hydration of a layered titanate. *J. Am. Chem. Soc.* **1998**, *120* (19), 4682−4689.

(10) Kayano, M.; Ogawa, M. Preparation of large platy particles of Co-Al layered double hydroxides. *Clays Clay Miner.* **2006**, *54* (3), 382−389.

(11) Arai, Y.; Ogawa, M. Preparation of Co-Al layered double hydroxides by the hydrothermal urea method for controlled particle size. *Appl. Clay Sci.* **2009**, *42* (3−4), 601−604.

(12) Yao, K.; Taniguchi, M.; Nakata, M.; Takahashi, M.; Yamagishi, A. Electrochemical scanning tunneling microscopy observation of ordered surface layers on an anionic clay-modified electrode. *Langmuir* **1998**, *14* (10), 2890−2895.

(13) Liu, X. H.; Ma, R. Z.; Bando, Y.; Sasaki, T. Layered Cobalt Hydroxide Nanocones: Microwave-Assisted Synthesis, Exfoliation, and Structural Modification. *Angew. Chem., Int. Ed.* **2010**, *49* (44), 8253−8256.

(14) Cai, H.; Hillier, A. C.; Franklin, K. R.; Nunn, C. C.; Ward, M. D. Nanoscale Imaging of Molecular Adsorption. *Science* **1994**, *266* (5190), 1551−1555.

(15) Costantino, U.; Marmottini, F.; Nocchetti, M.; Vivani, R. New synthetic routes to hydrotalcite-like compounds - Characterisation and properties of the obtained materials. *Eur. J. Inorg. Chem.* **1998**, No. 10, 1439−1446.

(16) Ogawa, M.; Kaiho, H. Homogeneous precipitation of uniform hydrotalcite particles. *Langmuir* **2002**, *18* (11), 4240−4242.

(17) Benito, P.; Herrero, M.; Barriga, C.; Labajos, F. M.; Rives, V. Microwave-assisted homogeneous precipitation of hydrotalcites by urea hydrolysis. *Inorg. Chem.* **2008**, *47* (12), 5453−5463.

(18) Jobbagy, M.; Blesa, M. A.; Regazzoni, A. E. Homogeneous precipitation of layered Ni(II)-Cr(III) double hydroxides. *J. Colloid Interface Sci.* **2007**, *309* (1), 72−77.

(19) Oh, J. M.; Hwang, S. H.; Choy, J. H. The effect of synthetic conditions on tailoring the size of hydrotalcite particles. *Solid State Ionics* **2002**, *151* (1−4), PII S0167−2738(02)00725−7.

(20) Iyi, N.; Sasaki, T. Decarbonation of MgAl-LDHs (layered double hydroxides) using acetate-buffer/NaCl mixed solution. *J. Colloid Interface Sci.* **2008**, *322* (1), 237−245.

(21) Iyi, N.; Matsumoto, T.; Kaneko, Y.; Kitamura, K. Deintercalation of carbonate ions from a hydrotalcite-like compound: Enhanced decarbonation using acid-salt mixed solution. *Chem. Mater.* **2004**, *16* (15), 2926−2932.

(22) Iyi, N.; Yamada, H.; Sasaki, T. Deintercalation of carbonate ions from carbonate-type layered double hydroxides (LDHs) using acid-alcohol mixed solutions. *Appl. Clay Sci.* **2011**, *54* (2), 132−137.

(23) Iyi, N.; Yamada, H. Efficient decarbonation of carbonate-type layered double hydroxide (CO_3^{2-}LDH) by ammonium salts in alcohol medium. *Appl. Clay Sci.* **2011**, *65*−*66*, 121−127.

(24) Antonyraj, C. A.; Koilraj, P.; Kannan, S. Synthesis of delaminated LDH: A facile two step approach. *Chem. Commun.* **2010**, *46* (11), 1902−1904.

(25) Iyi, N.; Matsumoto, T.; Kaneko, Y.; Kitamura, K. A novel synthetic route to layered double hydroxides using hexamethylenetetramine. *Chem. Lett.* **2004**, *33* (9), 1122−1123.

(26) Brönsted, J. N.; Kilpatrick, M.; Kilpatrick, M. Kinetic studies on ethylene oxides. *J. Am. Chem. Soc.* **1929**, *51*, 428−461.

(27) Parker, R. E.; Isaacs, N. S. Mechanisms of Epoxide Reactions. *Chem. Rev.* **1959**, *59* (4), 737−799.

(28) Cui, H. T.; Zayat, M.; Levy, D. Controlled homogeneity of the precursor gel in the synthesis of $SrTiO_3$ nanoparticles by an epoxide assisted sol-gel route. *J. Non-Cryst. Solids* **2007**, *353* (11−12), 1011−1016.

(29) Cui, H. T.; Zayat, M.; Levy, D. A chemical strategy to control the shape of oxide nanoparticles. *J. Nanopart. Res.* **2009**, *11* (6), 1331−1338.

(30) Gash, A. E.; Tillotson, T. M.; Satcher, J. H.; Poco, J. F.; Hrubesh, L. W.; Simpson, R. L. Use of epoxides in the sol-gel synthesis of porous iron(III) oxide monoliths from Fe(III) salts. *Chem. Mater.* **2001**, *13* (3), 999−1007.

(31) Gash, A. E.; Tillotson, T. M.; Satcher, J. H.; Hrubesh, L. W.; Simpson, R. L. New sol-gel synthetic route to transition and main-group metal oxide aerogels using inorganic salt precursors. *J. Non-Cryst. Solids* **2001**, *285* (1−3), 22−28.

(32) Gash, A. E.; Satcher, J. H.; Simpson, R. L. Monolithic nickel(II)-based aerogels using an organic epoxide: the importance of the counterion. *J. Non-Cryst. Solids* **2004**, *350*, 145−151.

(33) Gash, A. E.; Satcher, J. H.; Simpson, R. L. Strong akaganeite aerogel monoliths using epoxides: Synthesis and characterization. *Chem. Mater.* **2003**, *15* (17), 3268−3275.

(34) Zhang, H. D.; Li, B.; Zheng, Q. X.; Jiang, M. H.; Tao, X. T. Synthesis and characterization of monolithic Gd_2O_3 aerogels. *J. Non-Cryst. Solids* **2008**, *354* (34), 4089−4093.
(35) Ehrenberg, L.; Hussain, S. Genetic Toxicity of Some Important Epoxides. *Mutat. Res.* **1981**, *86* (1), 1−113.
(36) Bi, S. P.; Wang, C. Y.; Cao, Q.; Zhang, C. H. Studies on the mechanism of hydrolysis and polymerization of aluminum salts in aqueous solution: correlations between the ″Core-links″ model and ″Cage-like″ Keggin-Al-13 model. *Coord. Chem. Rev.* **2004**, *248* (5−6), 441−455.
(37) Vermeulen, A. C.; Geus, J. W.; Stol, R. J.; Debruyn, P. L. Hydrolysis-Precipitation Studies of Aluminum (III) Solutions 0.1. Titration of Acidified Aluminum Nitrate Solutions. *J. Colloid Interface Sci.* **1975**, *51* (3), 449−458.
(38) Stol, R. J.; Vanhelden, A. K.; Debruyn, P. L. Hydrolysis-Precipitation Studies of Aluminum (3) Solutions 0.2. Kinetic Study and Model. *J. Colloid Interface Sci.* **1976**, *57* (1), 115−131.
(39) Boclair, J. W.; Braterman, P. S. Layered double hydroxide stability. 1. Relative stabilities of layered double hydroxides and their simple counterparts. *Chem. Mater.* **1999**, *11* (2), 298−302.
(40) Parks, G. A. The isoelectric points of solid oxides, solid hydroxides, and aqueous hydroxo complex systems. *Chem. Rev.* **1965**, *65* (2), 177−198.
(41) Jobbagy, M.; Regazzoni, A. E. Dissolution of nano-size Mg-Al-Cl hydrotalcite in aqueous media. *Appl. Clay Sci.* **2011**, *51* (3), 366−369.
(42) Iyi, N.; Fujii, K.; Okamoto, K.; Sasaki, T. Factors influencing the hydration of layered double hydroxides (LDHs) and the appearance of an intermediate second staging phase. *Appl. Clay Sci.* **2007**, *35* (3−4), 218−227.
(43) Hibino, T.; Ohya, H. Synthesis of crystalline layered double hydroxides: Precipitation by using urea hydrolysis and subsequent hydrothermal reactions in aqueous solutions. *Appl. Clay Sci.* **2009**, *45* (3), 123−132.
(44) Scheidegger, A. M.; Lamble, G. M.; Sparks, D. L. Spectroscopic evidence for the formation of mixed-cation hydroxide phases upon metal sorption on clays and aluminum oxides. *J. Colloid Interface Sci.* **1997**, *186* (1), 118−128.
(45) d'Espinose De La Caillerie, J. B.; Kermarec, M.; Clause, O. Impregnation of gamma-alumina with Ni(II) or Co(II) ions at neutral pH: Hydrotalcite-type coprecipitate formation and characterization. *J. Am. Chem. Soc.* **1995**, *117* (46), 11471−11481.
(46) d'Espinose De La Caillerie, J. B.; Clause, O. Promotion of gamma-alumina dissolution by metal ions during impregnation. Thermal stability of the formed coprecipitates. *Stud. Surf. Sci. Catal.* **1996**, *101 B*, 1321−1330.
(47) Hiemstra, T.; Yong, H.; Van Riemsdijk, W. H. Interfacial charging phenomena of aluminum (hydr)oxides. *Langmuir* **1999**, *15* (18), 5942−5955.
(48) Kosmulski, M. pH-dependent surface charging and points of zero charge III. Update. *J. Colloid Interface Sci.* **2006**, *298* (2), 730−741.
(49) Kosmulski, M.; Plak, A. Surface charge of anatase and alumina in mixed solvents. *Colloids Surf., A: Physicochem. Eng. Aspects* **1999**, *149* (1−3), 409−412.
(50) Yang, Y.; Zhao, X.; Zhu, Y.; Zhang, F. Transformation mechanism of magnesium and aluminum precursor solution into crystallites of layered double hydroxide. *Chem. Mater.* **2012**, *24* (1), 81−87.
(51) Okamoto, K.; Iyi, N.; Sasaki, T. Factors affecting the crystal size of the MgAl-LDH (layered double hydroxide) prepared by using ammonia-releasing reagents. *Appl. Clay Sci.* **2007**, *37* (1−2), 23−31.
(52) Lang, K.; Kubat, P.; Mosinger, J.; Bujdak, J.; Hof, M.; Janda, P.; Sykora, J.; Iyi, N. Photoactive oriented films of layered double hydroxides. *Phys. Chem. Chem. Phys.* **2008**, *10* (30), 4429−4434.
(53) Yan, D. P.; Lu, J.; Wei, M.; Evans, D. G.; Duan, X. Sulforhodamine B Intercalated Layered Double Hydroxide Thin Film with Polarized Photoluminescence. *J. Phys. Chem. B* **2009**, *113* (5), 1381−1388.